Am J Physiol Cell Physiol 297: C188–C197, 2009.
First published May 13, 2009; doi:10.1152/ajpcell.00052.2009.

Identification of the large-conductance background K^+ channel in mouse B cells as TREK-2

Haifeng Zheng,[1] Joo Hyun Nam,[1] Bo Pang,[1] Dong Hoon Shin,[1] Ji Seon Kim,[1,4] Yang-Sook Chun,[1,4] Jong-Wan Park,[2,4] Hyowon Bang,[5] Woo Kyung Kim,[6] Yung E. Earm,[1] and Sung Joon Kim[1,3,4]

[1]*Department of Physiology,* [2]*Department of Pharmacology,* [3]*Kidney Research Institute,* [4]*Ischemic/Hypoxic Disease Institute, Seoul National University College of Medicine, Seoul;* [5]*Department of Physiology, Chung-Ang University College of Medicine, Seoul; and* [6]*Department of Internal Medicine, Dongguk University College of Medicine, Kyungpook, Korea*

Submitted 28 January 2009; accepted in final form 10 May 2009

Zheng H, Nam JH, Pang B, Shin DH, Kim JS, Chun YS, Park JW, Bang H, Kim WK, Earm YE, Kim SJ. Identification of the large-conductance background K^+ channel in mouse B cells as TREK-2. *Am J Physiol Cell Physiol* 297: C188–C197, 2009. First published May 13, 2009; doi:10.1152/ajpcell.00052.2009.—Mouse B cells and their cell line (WEHI-231) express large-conductance background K^+ channels (LK_{bg}) that are activated by arachidonic acids, characteristics similar to TREK-2. However, there is no evidence to identify the molecular nature of LK_{bg}; some properties of LK_{bg} were partly different from the reported results of TREK type channels. In this study, we compared the properties of cloned TREK-2 and LK_{bg} in terms of their sensitivities to ATP, phosphatidylinositol 4,5-bisphosphate (PIP_2), intracellular pH (pH_i), and membrane stretch. Similar to the previous findings of LK_{bg}, TREK-2 showed spontaneous activation after membrane excision (i-o patch) and were inhibited by MgATP or by PIP_2. The inhibition by MgATP was prevented by wortmannin, suggesting membrane-delimited regulation of TREKs by phosphoinositide (PI) kinase. The same was observed with the property of LK_{bg}; the activation of TREK-2 by membrane stretch was suppressed by U73122 (PLC inhibitor). As with the known properties of TREK-2, LK_{bg} were activated by acidic pH_i and inhibited by PKC activator. Finally, we confirmed the expression of TREK-2 in WEHI-231 by using RT-PCR and immunoblot analyses. The amplitude of background K^+ current and the TREK-2 expression in WEHI-231 were commonly decreased by genetic knockdown of TREK-2 using small interfering RNA. The downregulation of TREK-2 attenuated Ca^{2+}-influx induced by arachidonic acid in WEHI-231. As a whole, these results strongly indicate that TREK-2 encodes LK_{bg} in mouse B cells. We also newly suggest that the low activity of TREK-2 in intact cells is due to the inhibition by intrinsic PIP_2.

K2P channel; arachidonic acid; PI kinase; membrane stretch; immune cells

K^+ CHANNELS determine the membrane potential and thereby regulate calcium signaling, proliferation, and apoptosis of lymphocytes (3, 7, 24, 25). In both B and T cells, voltage-dependent K^+ channels (e.g., Kv1.3) and intermediate conductance calcium-activated potassium channels (IKCa1) are expressed with distinct patterns depending on the stages of activation and differentiation (25, 28). The blockers of these K^+ channels have been suggested as potential immune suppressants (4, 14, 24).

Apart from Kv and IKCa1, we reported that mouse immature B cell line (WEHI-231) and primary splenic B cells express large-conductance background K^+ channels (LK_{bg}) (22, 23). The slope conductance of LK_{bg} was noticeably large; close to 320 pS at negative voltage ranges in divalent-free (DVF) symmetrical 145 mM K^+ conditions. Although the activity of LK_{bg} was very low in cell-attached (c-a) configuration, it increased dramatically after making inside-out (i-o) patches or by membrane stretch stimuli (22, 23). MgATP applied to the cytoplasmic side reversibly inhibited LK_{bg}, and the effect was blocked by phosphoinositide (PI) kinase inhibitors. Also, LK_{bg} were almost completely inhibited by phosphatidylinositol 4,5-bisphosphate (PIP_2) (22). Since PI-kinase produces PIP_2 by using MgATP and PIP, such results were consistent with a hypothetical model of membrane-delimited inhibition of LK_{bg} by PIP_2 generation. Another type of background K^+ channel with smaller conductance (~110 pS) was also observed in WEHI-231 cells. However, the medium conductance background K^+ channels (MK_{bg}) were far less frequently observed and were easily distinguishable from LK_{bg} by their smaller conductance and insensitivity to MgATP and PIP_2 (22).

A physiological role of LK_{bg} was demonstrated from the augmentation of arachidonic acid-induced Ca^{2+} influx by the concomitant activation of LK_{bg} and strong hyperpolarization (30). Although the voltage independence of LK_{bg} suggested an involvement of two-pore K^+ channel (KCNK) family, the molecular identity of LK_{bg} has been unsolved. The molecular sequences of cloned background-type K^+ channels, KCNK family, commonly show two pore domains in tandem. The mammalian KCNK consists of six subfamilies: TWIK, TREK, TASK, TALK, THIK, and TRESK (9, 20). Among them, TREK subfamily channels (TREK-1, TREK-2, and TRAAK) are relatively quiescent in basal states; they are strongly activated by physicochemical stimuli such as unsaturated fatty acids, membrane stretch, intracellular acidification, and heat (1, 18, 15). In contrast, the PKC- or PKA-dependent phoshorylation inhibits TREK-1 and -2 (8, 16).

LK_{bg} was the first characterized background K^+ channel in immune cells and appeared to be preferentially expressed in immature B cells (22, 30). Hence, clarifying the molecular identity of LK_{bg} might be useful to understand B cell development. The large conductance of LK_{bg} in DVF condition is similar to the conductance of TREK-2 in the same DVF condition (8). Also, LK_{bg} is activated by membrane stretch (23) and by unsaturated fatty acids (30).

In the previous studies of LK_{bg}, however, we hesitated to suggest the molecular identity of LK_{bg} as TREK-2 because the reported PIP_2 sensitivity of TREK channel (TREK-1) at that time was opposite to that of LK_{bg}; activation by PIP_2 in TREK-1 (5, 19), whereas inhibition in LK_{bg} (22). In a more

Address for reprint requests and other correspondence: S. J. Kim, Dept. of Physiology, Seoul National Univ. College of Medicine, 103 Daehangno, Jongno-gu, Seoul 110-799, Korea (E-mail: sjoonkim@snu.ac.kr).

Table 1. *Nucleotide sequences of the primers used for RT-PCR*

Protein (GeneBank No.)	Primer	Position*	Product Size	Sequence (5′ to 3′)
Mouse TREK-1	Forward	632	589bp	CCATCATCTTCATCCTGTTT
(NM_010607)	Reverse	1220		ATGACAGCTATGTCCTCACC
Mouse TREK-2	Forwarde	977	454bp	CAAAAGAAGAGGTTGGTGAG
(NM_029911)	Reverse	1430		GAGTAATTCCGGAAGGTTTT
Mouse TRAAK	Forward	241	365bp	AATAGCAGCAACCACTCATC
(NM_008431)	Reverse	605		TCTAACTTGCTCCAGCTCTC
Mouse β-actin	Forward	263	587bp	ACACCTTCTACAATGAGCTG
(NM_007393)	Reverse	849		CATGATGGAATTGAATGTAG

*Primer position from the primary translation site.

recent study, Chemin et al. (6) demonstrated dual effects of PIP_2 on TREK-1: activation by relatively low concentrations of PIP_2, whereas inhibition by high concentrations of PIP_2. Regarding the controversies in PIP_2 sensitity of TREK channels, we were attempted to further investigate and compare the properties of LK_{bg} and TREK-2.

Here we found that the cloned TREK-2 and TREK-1 were inhibited by membrane-delimited generation of PIP_2. The mechanosensitivity of TREK-2 was found to be due to the degradation of PIP_2 through PLC. In addition, we investigated the effects of pH_i on LK_{bg} activity. Finally, we confirmed the molecular expression of TREK-2 in WEHI-231 and then investigated the effects of TREK-2-specific small interfering RNA (siRNA) (siTREK-2) on the membrane current and Ca^{2+} signaling in WEHI-231 cells.

METHODS AND MATERIALS

Cells. WEHI-231 cells were grown in 25 mM HEPES-RPMI 1640 media (GIBCO, Grand Island, NY) supplemented with 10% (vol/vol) fetal bovine serum (Hyclone, Logan), 50 μM 2-mercaptoethanol (Sigma, St. Louis, MO), and 1% penicillin-streptomycin (GIBCO) at 37°C in 20% O_2-5% CO_2.

HEK293 cells permanently expressing rat TREK-1 (rTREK-1) and TREK-2 (rTREK-2) were produced as previously described (29). Briefly, rTREK-1 and rTREK2 in pcDNA3.1 were transfected into HEK-293 cells using Lipofectamine 2000 (LF2000, Invitrogen). At 48 h after transfection, the cells were passaged at a higher dilution (around 100 cells/100 mm culture dish) into fresh medium. The next day, medium was replaced by selection medium containing 1 μg/ml G418. Selection medium was replaced every 3∼4 days. After 4 wk, single colonies were isolated by adhering sterile cloning cylinders to the bottom of the dishes using silicon, and cells contained within each cylinder were isolated by adding 200 μl trypsin-EDTA (1:25) at 37°C for 5 min. Each clone was characterized for channel expression by patch clamp. Stably expressing cells were grown in Dulbecco's Modified Eagle's medium (GIBCO) supplemented with 10% (vol/vol) fetal bovine serum (Hyclone, Logan) and 1% penicillin-streptomycin (GIBCO) at 37°C in 20% O_2-10% CO_2.

Electrophysiology. Cells were transferred into a bath mounted on the stage of an inverted microscope (IX-70, Olympus, Osaka, Japan). The bath (∼0.15 ml) was superfused at 5 ml/min, and voltage-clamp experiments were performed at room temperature (22–25°C). Patch

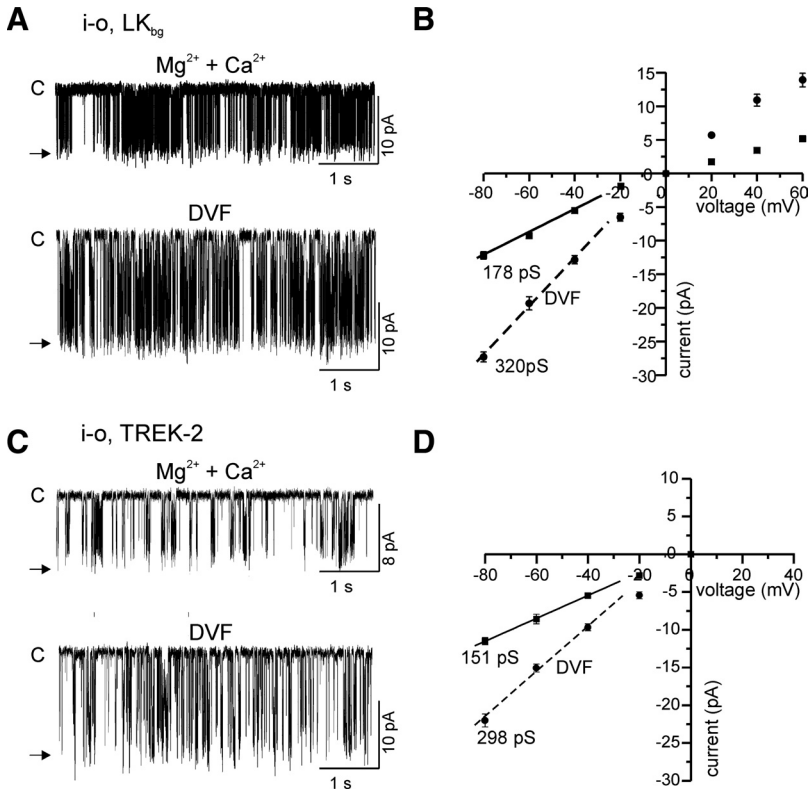

Fig. 1. Comparison of the unitary conductance of large conductance background K^+ channel (LK_{bg}) and TREK-2. *A* and *C*: representative traces of single channel currents at −60 mV in symmetrical KCl conditions of inside-out (i-o) recording at holding voltage of −60 mV with (*top*) or without Ca^{2+} and Mg^{2+} (divalent free, DVF, *bottom*) in the pipette solution. Arrows indicate the level of open channel current from the closed state (C). *B* and *D*: mean values of single channel amplitudes were plotted against the clamp voltage ($n = 6$). A linear fitting at negative voltages yields 178 pS (Ca^{2+}/Mg^{2+}) and 320 pS (DVF) for LK_{bg}, and 151 pS (Ca^{2+}/Mg^{2+}) and 298 pS (DVF) for TREK-2.

pipettes with a free-tip resistance of about 2.5 MΩ were connected to the head stage of a patch-clamp amplifier (Axopatch-1D, Axon Instruments, Foster City, CA). pCLAMP software v.9.2 and Digidata-1322A (Axon Instruments) were used to acquire data and apply command pulses. Whole cell currents and single channel activities were recorded at 10 kHz and were low-pass filtered at 0.5 and 2 kHz, respectively. The gain of amplifier for single channel recording was set at 50. Current traces were stored and analyzed using Clampfit v.9.2 and Origin v. 7.0 (Microcal, Northampton, MA). For comparison of whole cell currents between cells, the current amplitudes were normalized to the membrane area measured by electrical capacitance. Single channel data were analyzed to obtain total channel activities (NP_o) where N and P_o are the observed levels of channel opening and the open probability, respectively.

The pipette solution for whole cell patch clamp contained (in mM) 135 KCl, 6 NaCl, 10 HEPES, 3 MgATP, and 5 EGTA, with a pH of 7.2 (titrated with KOH), and the final $[K^+]$ reached about 140 meq/l. The normal bath solution for the whole cell patch clamp contained (in mM) 145 NaCl, 3.6 KCl, 1 $MgCl_2$, 1.3 $CaCl_2$, 5 glucose, and 10 HEPES, with a pH of 7.4 (titrated with NaOH). The pipette solution for c-a patch clamp contained (in mM) 140 KCl, 5 NaCl, and 5 HEPES with a pH of 7.4 (titrated with KOH). The pipette solution for i-o patch clamp and the bath solution for c-a and i-o patch clamp contained (in mM) 145 KCl, 1 EGTA, and 5 HEPES with a pH of 7.4 (titrated with KOH). Unless marked otherwise, most of the single channel recordings were performed with the DVF pipette solution. For acidic (pH 5.6 and 6.0) solution, HEPES was substituted by MES, and for basic (pH 8.0), HEPES was substituted by Tris. To examine the effects of mechanical stress on the activity of TREK-2 channels, we elicited membrane stretch by applying suction (negative pressure) through a sideport of the pipette holder to the patch membrane. The pressure was monitored with a manometer.

$[Ca^{2+}]_c$ measurement. Cells were harvested using the normal bath solution, loaded with fura-2 acetoxymethyl ester (4 μM, 30 min, 25°C), and washed twice with fresh solution. The fluorescence was monitored in a stirred quartz-microcuvette (1 ml) in the thermostated cell holder of fluorescence spectrophotometer (Photon Technology Instrument, Birmingham, NJ) at the wavelengths of 340 nm and 380 nm (excitation), and 510 nm (emission). Obtained results were calibrated by adding 5 μM ionomycin with 1.5 mM $CaCl_2$, which gives the maximum value of fluorescence ratio (340 nm/380 nm, R_{max}), and 10 mM EGTA, which gives the minimum value of fluorescence ratio (R_{min}). The $[Ca^{2+}]_c$ was calculated from the equation $[Ca^{2+}] = K_d \times b \times (R - R_{min})/(R_{max} - R)$, where K_d is the dissociation constant 224 nM for Fura-2 and b is the ratio of fluorescence excitation intensities at 380 nm under Ca^{2+}-free and Ca^{2+}-saturated condition.

RT-PCR. Total RNA was isolated from WEHI-231 cells by TRizol (Invitrogen, Carlsbad, CA). Mouse mRNAs of TREK-1, TREK-2, TRAAK, and β-actin were analyzed using a RT-PCR method. One microgram of RNA was reverse transcribed at 48°C for 20 min, and the produced cDNAs were amplified over 30 PCR cycles (94°C for 30 s, 52°C for 30 s, and 70°C for 30 s). To rule out the amplification of genomic DNAs, reverse transcriptase was omitted in the reaction mixture for RT-PCR (-RTase). The PCR products (5 μl) were electrophoresed on a 2% agarose gel at 100 V in a 1 × Tris-acetate-EDTA buffer and visualized using ethidium bromide. The nucleotide sequences of the primers and their position in the primary translation sites are summarized in Table 1.

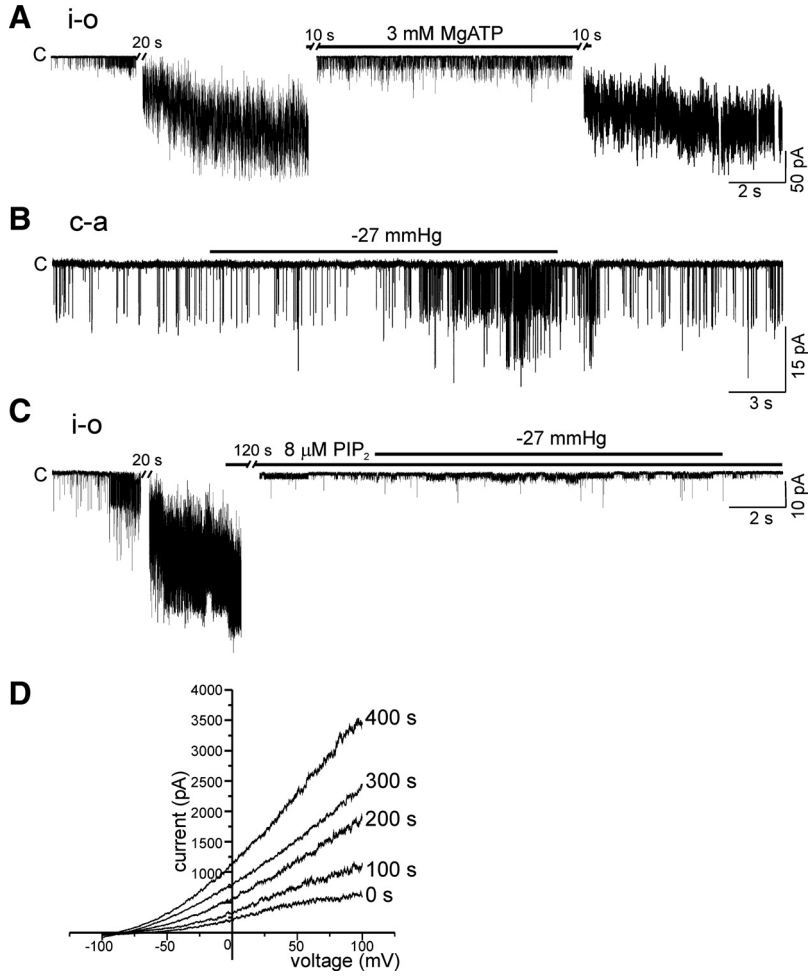

Fig. 2. Effects of intracellular MgATP and PIP_2 on TREK-2 activity. *A*: after making i-o configuration, spontaneous increase of inward K^+ current was observed (symmetrical KCl solution and −60 mV of clamp voltage). Bath application of 3 mM MgATP largely abolished the channel activity, and this was reversed by the washout of MgATP. C indicates closed level of channels. *B*: in cell-attached (c-a) condition with KCl pipette solution, the application of negative pressure (−27 mmHg) through the patch pipette activated TREK-2, and this was reversed by releasing the negative pressure. *C*: the spontaneously activated TREK-2 current by membrane excision was completely inhibited by 8 μM PIP_2. Under this condition, the membrane stretch (−27 mmHg) did not recover the channel activity. *D*: in the whole cell clamp conditions with MgATP-free KCl pipette solution, spontaneous increase of outward current was observed. The current-voltage (*I-V*) curves obtained by ramp-like pulses (from −100 to 100 mV) were overlaid and marked with the time after membrane break-in.

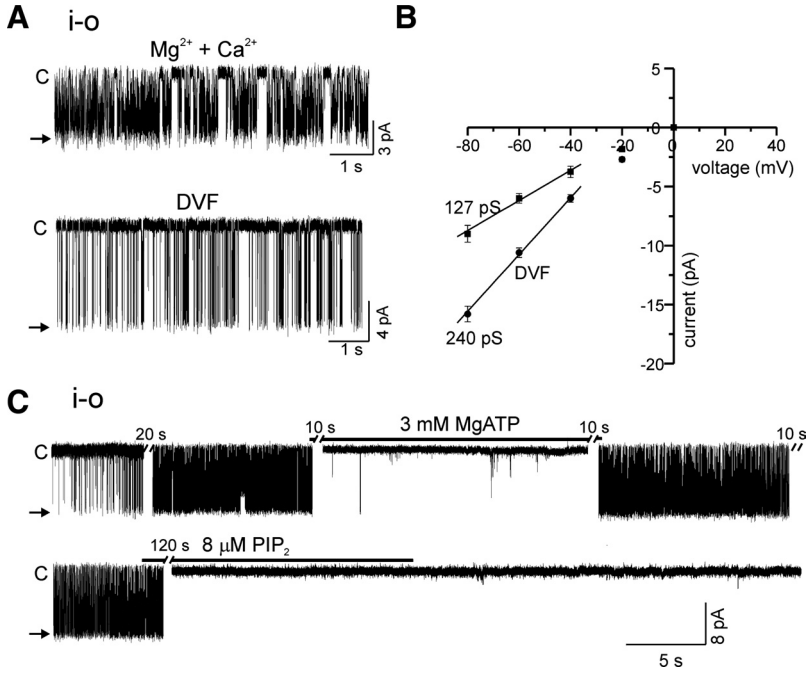

Fig. 3. Effects of extracellular divalent cations and intracellular MgATP on TREK-1. *A*: in symmetrical KCl (145 mM) conditions of i-o recording, single channels currents of TREK-1 were recorded in the absence (DVF) or presence of divalent cations (1 mM Mg^{2+} and Ca^{2+}) in the pipette solution. *B*: mean values of single channel amplitudes were plotted against the clamp voltage. A linear fitting at negative voltages yields 127 pS (Ca^{2+}/Mg^{2+}) and 240 pS (DVF). *C*: TREK-1 activated spontaneously after making i-o configuration and was inhibited by MgATP (3 mM) or by PIP_2 (8 μM).

Immunoblot. To determine the cellular levels of mouse TREK-2, 50 μg of cell lysate (membrane fraction) were separated on a 10% SDS-polyacrylamide gels, respectively, and transferred to an Immobilon-P membrane (Millipore, Billerica, MA). Membrane was blocked with 5% nonfat milk in Tris-buffered saline containing 0.1% Tween 20 (TTBS) at room temperature for 1 h, and immobilized proteins were incubated overnight 4°C with anti-TREK-2 (diluted 1:1,000, Santa Cruz, CA) antibody in 5% nonfat milk in TTBS. After being washed with three changes of TTBS, horseradish peroxidase-conjugated anti-goat (Santa Cruz), antiserum (GE Healthcare, NJ) was used as secondary antibodies diluted 1:5,000 in 5% nonfat in TTBS for 1 h. The antigen-antibody complexes were visualized by using Enhanced Chemiluminescence Plus Kit (GE Healthcare, NJ).

Transfection of siTREK-2. Synthetic siRNA targeting mouse TREK-2 (Santa Cruz Biochnology) and scrambled siRNA (scRNA) were transfected using AMAXA nucleofector and corresponding kit (AMAXA Biosystems, Cologne, Germany). Transfection protocol was performed following manufacture's instruction. Briefly, the cells were resuspended in the nucleofector solution. One hundred microliters of 2×10^6 to 5×10^6 /ml cells mixed with 2 μg of pmax green fluorescent protein (GFP) vector and siRNA (500 and 600 nM) were transferred to a cuvette and nucleofected with AMAXA nucleofector. The cells transfected with scRNA (Invitrogen) were used as negative controls. Forty-eight hours after the transfection, TREK-2 knockdown by the siRNA was verified using patch clamp, RT-PCR, and Western blot. The sequence of mouse TREK-2 siRNA was 5′-GGAAUUACUCUCUGGAUGA-3′.

Chemicals and drugs. The chemicals and drugs used in this study were purchased from Sigma (St. Louis, MO) except PIP_2 (Avanti Polar Lipids). To prepare PIP_2 solution, PIP_2 was dispersed by sonication in water at 2 mM for 30 min on ice and then kept at −20°C. PIP_2 was diluted to 8 μM in bath solution (for i-o patch) and sonicated 60 min in water on ice.

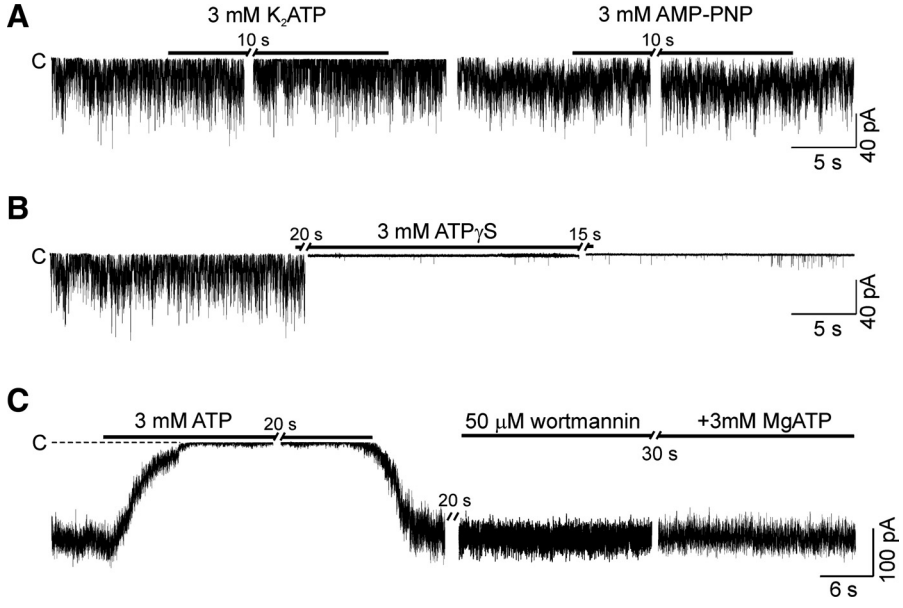

Fig. 4. Phosphoinositide (PI) kinase-dependent inhibition of TREK-2 by MgATP. The recordings were commonly obtained under the i-o patch-clamp conditions at −60 mV with symmetrical KCl (145 mM) solutions. *A*: bath application of K_2ATP (3 mM, *left trace*) and AMP-PNP (3 mM, *right trace*) had no effect on TREK-2 activity. *B*: representative traces of TREK-2 responses to ATPγS (3 mM) in i-o configurations. The inhibition of TREK-2 was not reversed by washout of ATPγS. *C*: after confirming the reversible inhibition by MgATP (3 mM), wortmannin (50 μM) was applied in the absence of MgATP. With wortmannin, MgATP had no inhibitory effect. Dotted line indicates closed level.

Data analysis and statistics. Data were represented as means ± SE. Student's *t*-test was used to test for significance at the level of 0.05.

RESULTS

Comparison between TREK-2 and LK_{bg}. The unitary slope conductance was compared in i-o recordings with symmetrical KCl (145 mM) condition. Single channel current amplitudes were measured at various clamp voltages with or without divalent cations in the pipette solution (Fig. 1, *A* and *C*). Because the current-voltage (*I-V*) curves showed weak inward rectification, the unitary slope conductance was obtained by linear fitting of three points at −80, −60, and −40 mV. With 1.3 mM Ca^{2+} and 1 mM Mg^{2+} ions in the pipette solution, the slope conductance of LK_{bg} was 178 pS and was increased to 320 pS in DVF condition (Fig. 1*B*). Similar to LK_{bg}, the slope conductance of TREK-2 was increased from 151 pS to 298 pS by removing divalent cations from the pipette solution (Fig. 1*D*).

Same with the properties of LK_{bg} (22, 23, 30), TREK-2 activated spontaneously after making i-o configuration, and the activation was almost completely reversed by 3 mM MgATP (Fig. 2*A*, $n = 15$) or by PIP_2 (Fig. 2, *A* and *C*, $n = 20$). The mechanosensitive activation of TREK-2, a well-known property of TREK family channels (15), was also confirmed by applying negative pressure (−27 mmHg) through the patch pipette in c-a recording (Fig. 2*B*). The stretch-induced activation of TREK-2 was blocked by the treatment with PIP_2 in i-o recording (Fig. 2*C*); same with the responses of LK_{bg} (23). Also, similar to the response of WEHI-231 and mouse splenic B cells (22, 23, 30), the whole cell membrane conductance of TREK-2 expressing HEK293 was spontaneously increased by dialyzing with ATP-free pipette

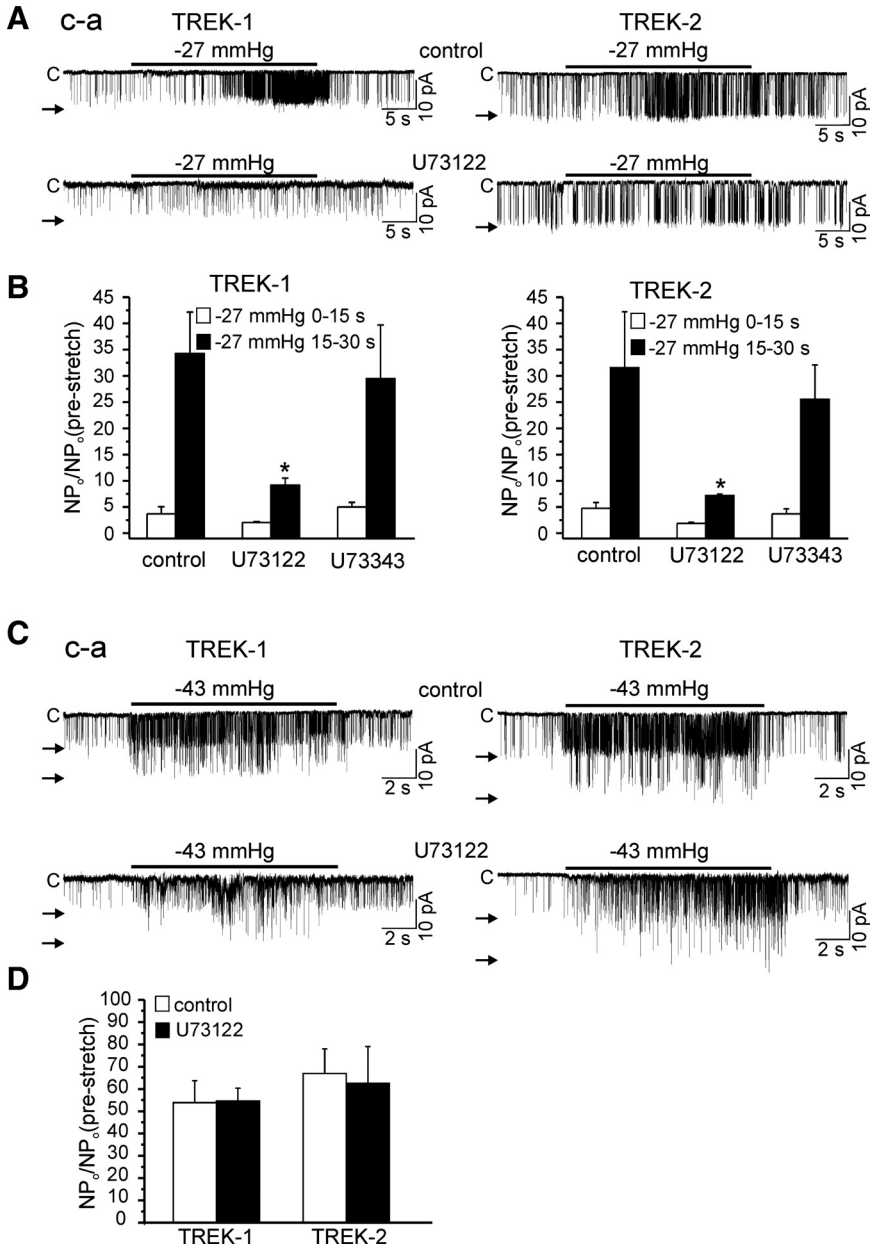

Fig. 5. Effects of PLC inhibitor on the mechanosensitive activation of TREK-1 and -2. After basal activities of TREK-1 and -2 in c-a configuration were confirmed, a relatively mild (−27 mmHg) or strong (−43 mmHg) suction was applied as indicated above each trace. *A*: both TREK-1 and -2 were slowly activated by −27 mmHg of suction (*top*), and these responses were significantly suppressed by the pretreatment with U73122 (2 μM, *bottom*). *B*: summaries of the changes in channel activity (NP_o) by relatively low membrane stretch (−27 mmHg) and the effects of pretreatment with U73122 (2 μM) or with U73343 (10 μM). In each patch, NP_o during the initial 15 s and the later 15 s of membrane stretch were normalized against the prestretch activity. The averaged values are shown as bar graphs ($n = 6$). *C*: representative traces of TREK-1 and TREK-2 responses to the higher level of membrane stretch (−43 mmHg). The pretreatment with U73122 did not block the activation of TREKs by the stronger negative pressure. Representative cases from five similar experiments are shown. *D*: summaries of the NP_o changes by relatively high membrane stretch (−43 mmHg) and the effects of pretreatment with U73122 (2 μM, $n = 5$).

solution. The whole cell *I-V* curve showed Ohmic relation and negative reversal potential, indicating the activation of TREK-2 (Fig. 2*D*, $n = 5$). Such increase of whole cell conductance was not observed with MgATP containing (3 mM) pipette solution (data not shown, $n = 5$). In i-o patches of WEHI-231 cells, it was notable that small-conductance channels were sometimes induced by PIP_2 treatment (Fig. 2*C*). These channels were not K^+ selective, and the expected unitary conductance was around 30 pS (ca. 2 pA at −60 mV, data not shown). Similar channel activity was also observed in c-a patches treated with PKC activator (Fig. 7*B*). We did not further investigate these small conductance channels here.

The effects of MgATP and PIP_2 on TREK-1 were also tested. The slope conductance of TREK-1 was smaller than TREK-2 and were increased from 127 to 240 pS in DVF

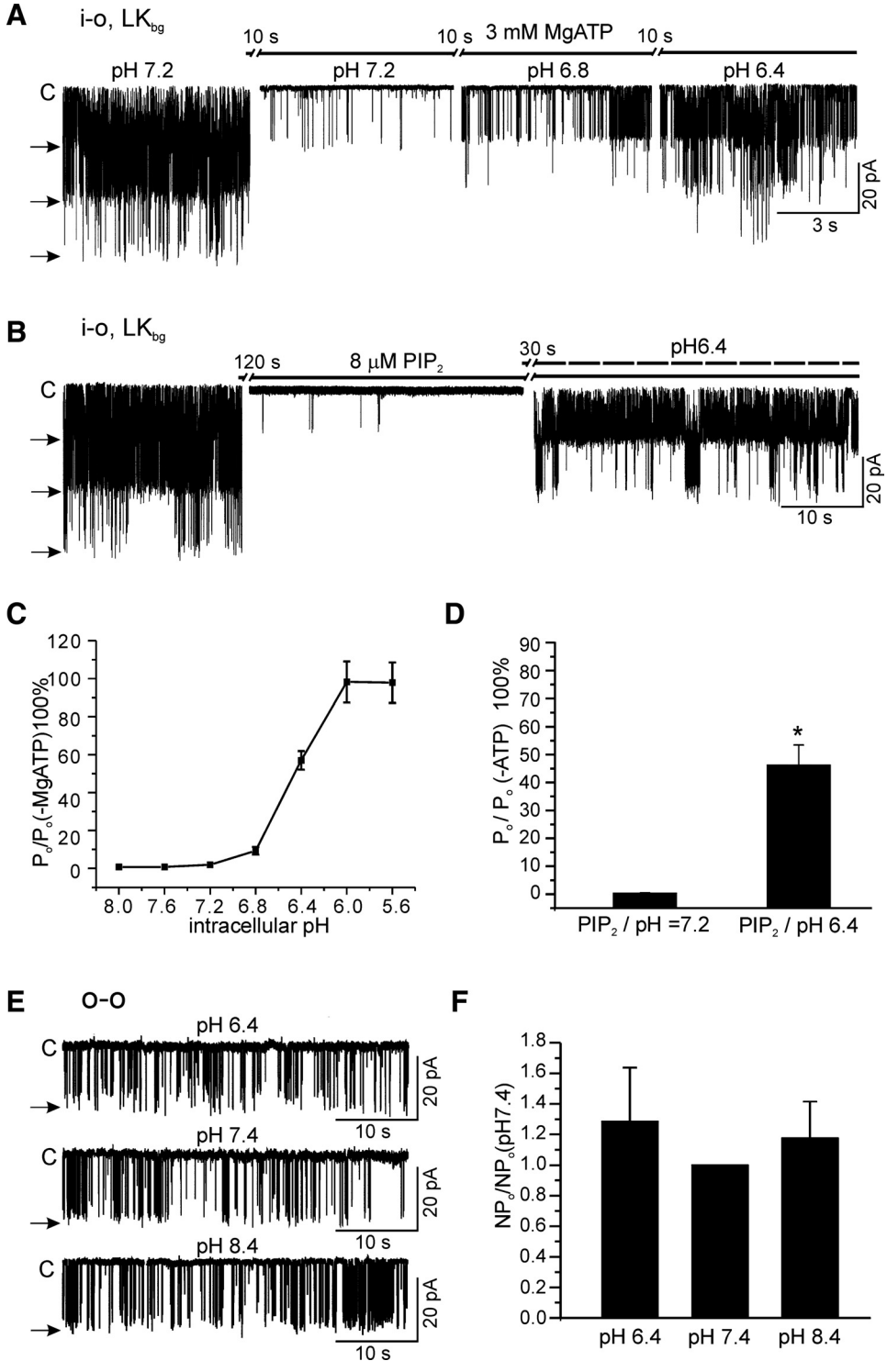

Fig. 6. Activation of LK_{bg} by acidic intracellular pH. *A*: in the i-o recordings from WEHI-231 cells, steady-state activity of LK_{bg} and its inhibition by 3 mM MgATP were confirmed (holding voltage, −60 mV). The acidification of intracellular solution (pH 6.8 and 6.4) reactivated LK_{bg}. *B*: inhibition LK_{bg} by PIP_2 (8 μM) was also reversed by acidic intracellular pH (6.4). *C*: in each patch, the open probability (P_o) of LK_{bg} in various pH with MgATP (3 mM) were normalized (%) to the maximum P_o obtained under the MgATP-free condition at pH 7.2. The means ± SE of normalized value were plotted against the tested pH ($n = 5$). *D*: bar graph summarizing the effect of acidic pH (6.4) on the PIP_2-inhibited LK_{bg}. The P_o at pH 7.2 and 6.4 with 8 μM PIP_2 was normalized (%) to the maximum P_o obtained under the MgATP-free condition at pH 7.2 ($n = 6$). $^*P < 0.05$ vs. control (pH 7.2). *E*: representative traces of the same outside-outside (o-o) patch from a WEHI-231 cell. LK_{bg} was identified from the characteristic large conductance (see arrows indicating the open level; holding voltage, −60 mV). pH of bath solution was indicated directly above each trace. *F*: changing pH of bath solution did not affect LK_{bg} activity. In each patch, NP_o of LK_{bg} at pH 6.4 and 8.4 were normalized to the control NP_o recorded at pH 7.4 and then averaged values are displayed ($n = 5$).

condition (Fig. 3, *A* and *B*, $n = 7$). Whereas the unitary conductance was smaller than TREK-2 and LK_{bg}, the spontaneous activation by i-o patch and the inhibition by MgATP or by PIP_2 were similarly observed (Fig. 3*C*, $n = 5$, respectively).

We then investigated the mechanism of TREK-2 inhibition by MgATP. After the steady-state activation of TREK-2 in i-o conditions, neither Mg^{2+}-free ATP (3 mM K_2ATP without Mg^{2+}, 0.1 mM EDTA included) nor AMP-PNP, a nonhydrolyzable form of ATP, affected the activity of TREK-2 (Fig. 4*A*, $n = 6$, respectively). In contrast, 3 mM ATPγS induced a nonreversible inhibition of TREK-2 (Fig. 4*B*, $n = 5$), indicating that phosphorylation process is involved. Wortmannin (50 μM), an inhibitor of PI-4 kinase as well as PI-3 kinase at this concentration, effectively prevented the inhibition of TREK-2 by MgATP (Fig. 4*C*, $n = 6$). Such results indicated that PIP_2 formation mediate the inhibitor effects of MgATP on TREK-2, same with the responses of LK_{bg} (22). The inhibition by MgATP and its prevention by wortmannin were also confirmed in TREK-1 (supplementary Fig. 1).

Activation by membrane stretch is the well-recognized property of TREKs. A previous study suggested that direct interactions between positively charged COOH-terminal domain and membrane phospholipid mediate the mechanosensitivity of TREK-1 (5). However, in another study of TREK-2 with deletion mutation in COOH-terminal region, the transmembrane domains also partly mediated the mechanosensitivity (17). In WEHI-231 B cells, we previously suggested that the membrane stretch-dependent activation of LK_{bg} is mediated by mechanosensitive PLCs hydrolyzing PIP_2 (23). Such "PLC hypothesis" of mechanosensitivity was tested in TREK-1 and TREK-2 by using a pharmacological inhibitor of PLC, U73122. In c-a conditions, negative pressure (−27 mmHg) through the patch pipette activated TREKs with some delay (15–20 s) to reach a steady-state (Fig. 5*A*, *top trace*). The pretreatment with U73122 (2 μM) largely prevented the activation (Fig. 5*A*, *bottom trace*). In contrast, U73343 (10 μM), a negative analogue of U73122, had no effect on the activation of TREKs by the negative pressure (−27 mmHg, original trace not shown here). The summarized responses were shown as bar graphs (Fig. 5*B*, $n = 6$). We also tested the effects of a higher level of negative pressure −43 mmHg. At the stronger membrane stretch, interestingly, the activation of TREKs was more immediate, and the activation by higher pressure was not effectively blocked by U73122 (Fig. 5, *C* and *D*, $n = 5$).

Effects of pH_i on LK_{bg}. Activation by acidic intracellular pH (pH_i) is a representative property of TREK-2 (1, 17, 18), which has not been tested in LK_{bg} yet. After the spontaneous full activation of LK_{bg} in i-o patch condition without ATP, neither acidification nor alkalinization affected the activity of LK_{bg} ($n = 5$ and 4, respectively, supplementary Fig. 2), Therefore, the effects of pH_i change on LK_{bg} was investigated under the inhibition by MgATP or by PIP_2 (Fig. 6). In the presence of 3 mM MgATP, LK_{bg} were reversibly activated by acidic pH_i (< 7.2), whereas not affected by alkaline pH_i (>7.2) (Fig. 6, *A* and *C*, $n = 5$). Even the strong inhibition by direct application of PIP_2 (8 μM) was reversed by acidic pH_i (Fig. 6, *B* and *D*, $n = 6$). In contrast, the changes in extracellular pH (pH_e) did not affect the LK_{bg} activity measured in outside-out (o-o) configuration with 3 mM MgATP in the pipette (Fig. 6, *E* and *F*, $n = 5$). In HEK293 cells overexpressing TREK-2, we also confirmed that activation by acidic pH_i was prominent after the inhibition of TREK-2 by MgATP (supplementary Fig. 3).

In addition to the effects of physicochemical conditions, we found that an application of PKC activator, phorbol myristic acetate (PMA 0.5 μM), inhibited LK_{bg} (Fig. 7). In c-a recordings of WEHI-231, some cases of LK_{bg} showed relatively high activities in control states, and the application of 0.5 μM PMA inhibited LK_{bg} to 11.9 ± 2.0% of control activity (Fig. 7*B*, $n = 6$), which was similar with the previous reports in TREK-2 (8, 16). The solvent for PMA stock solution (EtOH) alone had no effect on TREK-2 (supplementary Fig. 4).

Molecular biological identification of LK_{bg}. RT-PCR analysis of mRNAs obtained from WEHI-231 cells showed that the transcript of TREK-2, but neither TREK-1 nor TRAAK, is expressed (Fig. 8*A*). Also, an immunoblot assay using commercially available antibodies confirmed the expression of TREK-2 proteins in WEHI-231 cells (Fig. 8*C*). The knockdown of TREK-2 expression by transfection of mouse TREK-2-specific siRNAs markedly decreased the mRNAs as well as proteins of TREK-2 in WEHI-231 cells (Fig. 8, *B* and *C*). It was then examined whether the functional expression of LK_{bg} is affected by siTREK-2. In whole cell patch with MgATP-free pipette solution, spontaneous increase of background-type outward current was consistently observed in mock-transfected (scRNA) WEHI-231 cells (Fig. 8*D*, $n = 20$) as previously described (22). The steady-state outward currents were noticeably smaller in siTREK-2-treated WEHI-231 cells. The amplitudes at −50 mV normalized to membrane capacitance were 3.6 ± 1.6 and 0.9 ± 0.3 pA/pF in mock- and siTREK-2-transfected cells, respectively (Fig. 8*E*). In i-o patches, the presence of LK_{bg} was confirmed by characteristic large unitary currents of 20 pA at −60 mV and the inhibition by 3 mM

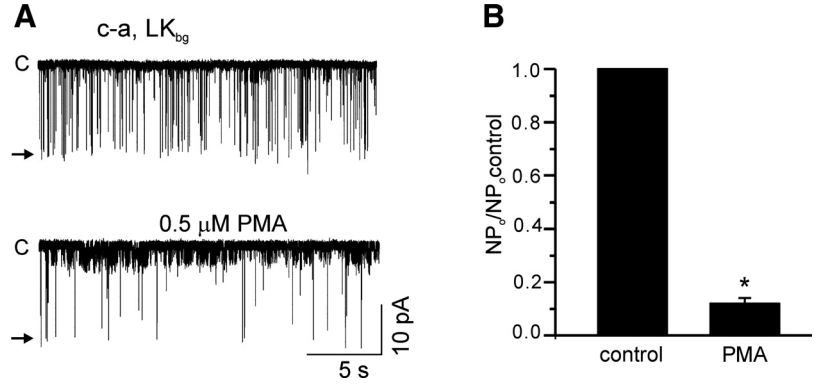

Fig. 7. Inhibition of LK_{bg} by PKC activator. *A*: representative traces showing the effects of phorbol myristic acetate (PMA) (0.5 μM) in c-a recording of LK_{bg} in WEHI-231 cells (holding voltage, −60 mV). *B*: summary of PMA on LK_{bg}. The total channel activity (NP_o) in the presence of PMA was normalized to the control activity in c-a recording (NP_o/NP_o control, $n = 6$). $^*P < 0.05$ vs. control.

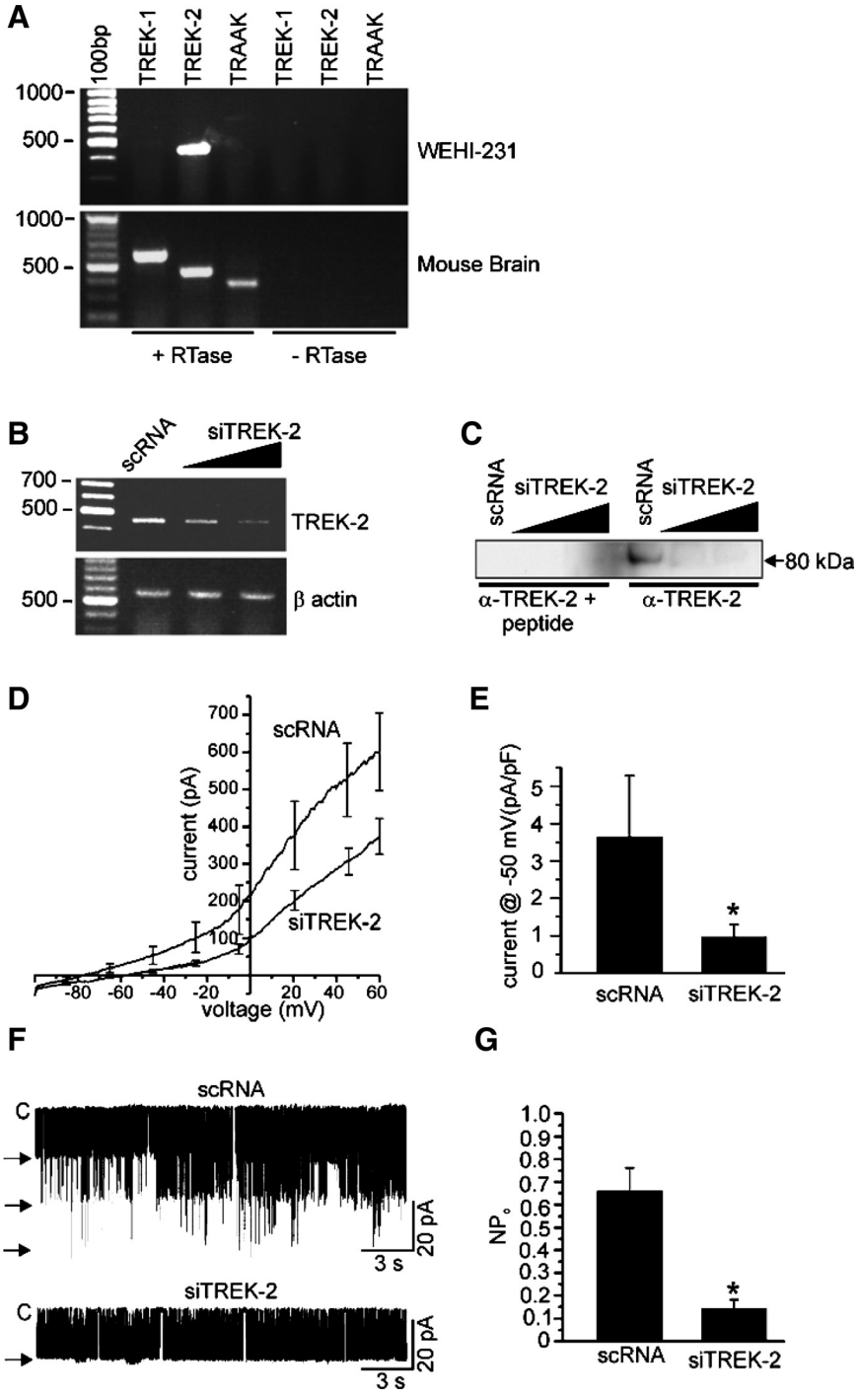

Fig. 8. Molecular identification of LK_{bg}. *A*: RT-PCR detection of mouse TREK-2 mRNA in WEHI-231 cells. Agarose gel electrophoresis of PCR products generated using specific primers for mouse TREK-1, TREK-2, and TRAAK. The first lane shows the molecular size marker (100 base pairs interval). In the absence of reverse transcriptase (−RTase) no PCR products were amplified. The expressions of TREK-1, -2, and TRAAK in mouse brain were confirmed (*bottom*), proving the validity of PCR primers for each channel. *B* and *C*: WEHI-231 cells were treated with 500 or 600 nM of small interfering TREK-2 (siTREK-2). As a control, scrambled siRNA (scRNA, 500 nM) was treated. Both RT-PCR analysis (*A*) and immunoblot analysis (*C*) showed decrease mRNAs and proteins for TREK-2 by the siTREK-2 treatment. In *B*, it was also confirmed that the PCR products of β actin were not affected by siTREK-2 transfection. In *C*, the effectiveness of TREK-2 antibodies (α-TREK-2) was confirmed by using blocking antigenic peptides; no immunoblot product in scRNA-treated cells in the left-most lane. *D*: effects of siTREK-2 treatment on the outward current of WEHI-231. MgATP-free pipette solution was used for the whole cell recording, and spontaneous increase of Ohmic outward current was observed. The means ± SE of steady-state *I-V* curves are shown in control (scRNA treated) and siTREK-2-treated WEHI-231 cells ($n = 20$, respectively). *E*: for each cell tested in *D* amplitude of outward current at −50 mV was normalized to the membrane capacitance (pA/pF) and the means ± SE were plotted ($n = 20$). $^*P < 0.05$ vs. scRNA. *F:* representative traces of LK_{bg} single channel currents (i-o patch) recorded in symmetrical KCl (145 mM) at −60 mV. *G*: summary of the total activities of LK_{bg} (NP_o) in scRNA and siTREK-2 treated WEHI-231 cells ($n = 50$, respectively). $^*P < 0.05$ vs. scRNA.

MgATP. We succeeded to record LK_{bg} in 32 patches of 50 trials (64%) in scRNA-transfected cells, but only 12 patches out of 50 trials (24%) in siTREK-2 transfected cells. The averaged net activities (NP_o) of LKbg were also markedly decreased in siTREK–treated cells (Fig. 8, *F* and *G*).

To investigate the physiological role of LK_{bg} (TREK-2), we compared the arachidonic acid-induced increase in $[Ca^{2+}]_c$ between the two groups of WEHI-231 cells. According to our previous study (30), arachidonic acid activated Ca^{2+}-permeable cation channels as well as LK_{bg} in WEHI-231 cells. The activated LK_{bg} would provide an electrical driving force for the Ca^{2+} influx. Consistent with such proposed role, the arachidonic acid-induced increase in $[Ca^{2+}]_c$ was significantly decreased in siTREK-2 transfected cells (Fig. 9, *A* and *B*).

DISCUSSION

The above results indicate that TREK-2 (KCNK10) encodes LK_{bg} in WEHI-231 cells, a well-known model of immature B cells. Apart from the molecular nature of the background-type K^+ channel in B cells, we also found that endogenously generated PIP_2 negatively regulates both TREK-2, which is

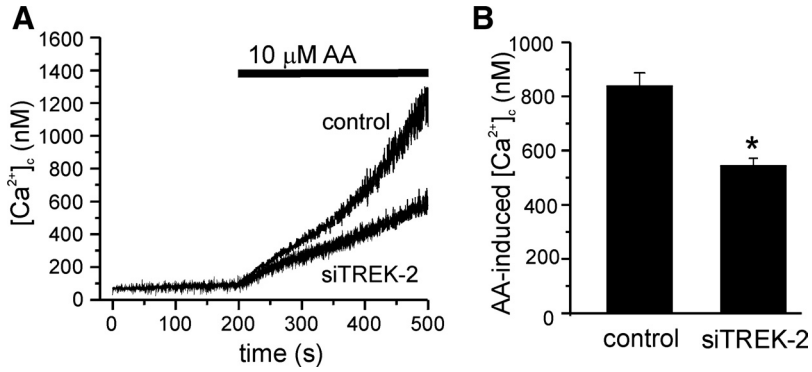

Fig. 9. Effects of siTREK-2 on arachidonic acid (AA)-induced augment of cytosolic $[Ca^{2+}]$ ($[Ca^{2+}]_c$). *A*: representative traces of the $[Ca^{2+}]_c$ of WEHI-231 cells and their response to AA (10 μM) are shown in control (sc RNA treated) and siTREK-2-treated WEHI-231 cells ($n = 7$, respectively). *B*: summary of $[Ca^{2+}]_c$ measured at 250 s of AA application to control and siTREK-2-treated WEHI-231 cells. $^*P < 0.05$ vs. control.

apparently antagonized by acidic pH_i. Also, the stretch-induced activation of TREK-2 might be partly mediated by mechanosensitive PLC activity by decreased PIP_2 level by hydrolysis. Although the inhibitory effects of PIP_2 and the PLC-mediated mechanosensitivtiy were previously demonstrated in the LK_{bg} of the mouse B cells (22, 23), the corresponding properties of transfected TREK-2 were novel findings, especially considering the controversies on the PIP_2-sensitivity of TREKs (see below).

Regulation of TREKs by PIP_2. In the control c-a recording without specific stimuli, the basal activities of TREKs and LK_{bg} were commonly low. The activities increased spontaneously by membrane excision (i-o patch), which was inhibited by MgATP or ATPγS. Because neither AMP-PNP nor Mg^{2+}-free ATP (K_2ATP) showed such inhibitory effects, it was strongly suggested that phosphorylation process is involved in the inhibition of TREK-2. Because the inhibition by MgATP was prevented by the pretreatment with wortmannin, we interpret that the low basal activity of TREKs in HEK293 is due to the tonic inhibitory effects of intrinsic PIP_2; we noted same with the previously reported membrane delimited regulation of LK_{bg} by PIP_2 metabolism (22).

PIP_2 is well recognized as a physiological regulator of ion channels and transporters (10, 12, 27). Except cyclic nucleotide-gated cation channels and inositol 1,4,5-trisphosphate receptor channels, most of the PIP_2-sensitive ion channels are positively regulated by PIP_2 (27). Although the initial study of TREK-1 showed activation by PIP_2 in primary neuronal cells (5), the same group revisited this issue and found mixed dual effects on TREK-1 in the recent study (6). However, in our hands, both TREKs and LK_{bg} were always inhibited by PIP_2 from micromolar concentrations. Unfortunately, there is yet no clear explanation about the differential responses between studies. A plausible hypothesis is that the basal level of membrane PIP_2 might be different depending on the cell type. In the present study, we tested HEK293 and WEHI-231 cells, whereas Chemin et al. (5, 6) and Lopez et al. (19) used primary neuronal cells, COS-7, and Xenopus oocytes expressing TREK-1. Further investigation with various forms of point mutations is still necessary to elucidate the PIP_2-dependent regulation of TREKs.

Mechanosensitivity of TREKs and PLC-PIP_2 signaling. The model of tonic inhibition by endogenous PIP_2 suggested that the hydrolysis by PLC might activate TREKs. According to our previous study, the membrane stretch-dependent activation of LK_{bg} (TREK-2) was mediated by mechanosensitive PLC-γ2 (23). In the present study, we observed similar results in TREK-1 and TREK-2 expressing HEK293 cells where the activation by relatively mild membrane stretch (−27 mmHg) was blocked by the pretreatment with PLC inhibitor U73122 (Fig. 5). For the activation by a relatively low level of negative pressure, −27 mmHg, it took tens of seconds to reach a steady-state activation of TREKs (Fig. 5, *A* and *B*), which seemed to be consistent with the putative enzymatic actions. However, when the negative pressure was raised to a higher level (−43 mmHg), the activation of TREKs were rapidly induced and uninhibited by U73122. Such results might suggest that more than single mechanisms with differential sensitivities to mechanical stimuli are involved; low threshold activation by mechanosensitive hydrolysis of PIP_2 while higher threshold activation by direct interaction between COOH-terminal region of TREKs and membrane phospholipids (5).

A model of TREK-1 regulation suggested that electrostatic interaction between COOH-terminal region and PIP_2 in the membrane inner leaflet mediates the mechanosensitive activation. In addition, the neutralization of positive amino acid in COOH-terminal (Glu306) by acidic pH_i greatly facilitated the mechanosensitivity and thereby activated TREK-1 in i-o patches (11). As mentioned above, however, the direction of PIP_2 action on TREKs are still controversial depending on the reports. In this regard, the activation of LK_{bg} (i.e., TREK-2) by acidic pH_i might be mediated also by a disinhibitory effects on the interaction between TREK-2 and PIP_2. No further effect of pH_i in the absence of MgATP is also suggestive of such hypothesis (supplementary Fig. 2).

Expression of K2P channels in immune system. One of the early cloning studies of TREK-2 demonstrated the expression of TREK-2 mRNAs in the spleen of rats (1). Nevertheless, the functional expression of K2P (KCNK) channels in the immune cells has been rarely investigated. Except our own reports, only two studies have detected the expression of K2P channels (TASK and TRESK) in T lymphocytes (21, 26).

TREK-2 might play a role in the regulation of immune responses. Up to now, the pathophysiological roles of TREKs have been mainly suggested in terms of neuropathic pain and brain ischemia related with inflammatory conditions (11, 13). Actually, the various stimuli activating TREKs are reminiscent of inflammatory environment (i.e., acidic pH, arachidonic acid, heat, etc.). Although not shown here directly, a high sensitivity of LK_{bg} to temperature was also confirmed in WEHI-231 cells (supplementary Fig. 5).

The resting membrane potentials of B cells recorded in the whole cell clamp configuration showed moderately depolarized values (ca. −40 mV) and were strongly hyperpolarized close to

−90 mV by the LK_{bg} stimulators such as arachidonic acids (30). The membrane hyperpolarization by TREK-2 activation would provide electrical driving force for Ca^{2+} influx, a critical signal for immunological responses. In this respect, the augmentation of Ca^{2+} signaling would be the most important role of K^+ channels in lymphocytes, and our study also demonstrated such example (Fig. 9, *A* and *B*).

Another common role of K^+ channel is the regulation of cell volume. In general, the continuous efflux of K^+ is accompanied by Cl^- efflux and resultantly relieves the osmotic burdening of cell swelling. It is also suggested that an excessive activation of K^+ efflux primarily decreased intracellular $[K^+]$ and cell volume, which might trigger the apoptotic signaling cascades (2). In the development and maturation processes of lymphocytes, most of self-reactive immature cells are removed by apoptosis. In this respect, the higher activity of LK_{bg} (TREK-2) in the immature B cell line (WEHI-231) or splenic B cells with immature B cell marker (30) might give an intriguing implication.

In summary, we suggest that the molecular nature of LK_{bg} in mouse B cells as TREK-2. The functional identification and cloning of K2P channels in lymphocytes have been only recently started. Considering the variety of regulatory factors for K2P channels including TREK-2, the investigation of their physiological/immunological roles might provide intriguing possibilities of modulating the functions of immune cell.

ACKNOWLEDGMENTS

We appreciate helpful discussion and comment from Dr. Dawon Kang.

GRANTS

This work was supported by the Korea Science and Engineering Foundation (KOSEF) grant funded by the Korea government (MEST) (No. R01-2008-000-11203-0 and R11-2007-040-01003-0).

REFERENCES

1. **Bang H, Kim Y, Kim D.** TREK-2, a new member of the mechanosensitive tandem pore K+ channel family. *J Biol Chem* 275: 17412–17419, 2000.
2. **Bortner CD, Cidlowski JA.** Cell shrinkage and monovalent cation fluxes: role in apoptosis. *Arch Biochem Biophys* 462: 176–188, 2007.
3. **Cahalan MD, Wulff H, Chandy KG.** Molecular properties and physiological roles of ion channels in the immune system. *J Clin Immunol* 21: 235–252, 2001.
4. **Chandy KG, Wulff H, Beeton C, Pennington M, Gutman GA, Cahalan MD.** K^+ channels as targets for specific immunomodulation. *Trends Physiol Sci* 25: 280–289, 2007.
5. **Chemin J, Patel AJ, Duprat F, Lauritzen I, Lazdunski M, Honore E.** A phospholipid sensor controls mechanogating of the K^+ channel TREK-1. *EMBO J* 24: 44–53, 2005.
6. **Chemin J, Patel AJ, Duprat F, Sachs F, Lazdunski M, Honore E.** Up- and down-regulation of the mechano-gated K(2P) channel TREK-1 by PIP_2 and other membrane phospholipids. *Pflügers Arch* 455: 97–103, 2007.
7. **Gallo EM, Cante-Barrett K, Crabtree GR.** Lymphocyte calcium signaling from membrane to nucleus. *Nat Immunol* 7: 25–32, 2006.
8. **Gu W, Schlichthörl G, Hirsch JR, Engels H, Karschin C, Karschin A, Derst C, Steinlein OK, Daut J.** Expression pattern and functional characteristics of two novel splice variants of the two-pore-domain potassium channel TREK-2. *J Physiol* 539: 657–668, 2002.
9. **Gurney A, Manoury B.** Two-pore potassium channels in the cardiovascular system. *Eur Biophys J* 1: DOI 10.1007/s00249-008-0326-8, 2008.
10. **Hilgemann DW, Feng S, Nasuhoglu C.** The complex and intriguing lives of PIP_2 with ion channels and transporters. *Sci STKE* 2001: RE19, 2001.
11. **Honore E.** The neuronal background K_{2P} channels: focus on TREK1. *Nat Rev Neurosci* 8: 251–261, 2007.
12. **Huang CL.** Complex roles of PIP_2 in the regulation of ion channels and transporters. *Am J Physiol Renal Physiol* 293: F1761–F1765, 2007.
13. **Huang D, Yu B.** Recent advance and possible future in TREK-2: A two-pore potassium channel may involved in the process of NPP, brain ischemia and memory impairment. *Med Hypotheses* 70: 618–624, 2008.
14. **Jensen BS, Hertz M, Christophersen P, Madsen LS.** The Ca^{2+}-activated K^+ channel of intermediate conductance: a possible target for immune suppression. *Expert Opin Ther Targets* 6: 623–636, 2002.
15. **Kang D, Choe C, Kim D.** Thermosensitivity of the two-pore domain K^+ channels TREK-2 and TRAAK. *J Physiol* 564: 103–16, 2005.
16. **Kang D, Han J, Kim D.** Mechanism of inhibition of TREK-2 (K2P10.1) by the Gq-coupled M3 muscarinic receptor. *Am J Physiol Cell Physiol* 291: C649–C656, 2006.
17. **Kim Y, Gnatenco C, Bang H, Kim D.** Localization of TREK-2 K^+ channel domains that regulate channel kinetics and sensitivity to pressure, fatty acids and pH_i. *Pflügers Arch* 442: 952–960, 2001.
18. **Lesage F, Terrenoire C, Romey G, Lazdunski M.** Human TREK2, a 2P domain mechano-sensitive K^+ channel with multiple regulations by polyunsaturated fatty acids, lysophospholipids, and G_s, G_i, and G_q protein-coupled receptors. *J Biol Chem* 275: 28398–28405, 2000.
19. **Lopes CM, Rohács T, Czirják G, Balla T, Enyedi P, Logothetis DE.** PIP_2 hydrolysis underlies agonist-induced inhibition and regulates voltage gating of two-pore domain K^+ channels. *J Physiol* 564: 117–129, 2005.
20. **Lotshaw DP.** Biophysical, pharmacological, and functional characteristics of cloned and native mammalian two-pore domain K^+ channels. *Cell Biochem Biophys* 47: 209–256, 2007.
21. **Meuth SG, Bittner S, Meuth P, Simon OJ, Budde T, Wiendl H.** TWIK-related acid-sensitive K+ channel 1 (TASK1) and TASK3 critically influence T lymphocyte effector functions. *J Biol Chem* 283:14559–145570, 2008.
22. **Nam JH, Woo JE, Uhm DY, Kim SJ.** Membrane-delimited regulation of background K^+ channels by MgATP in murine immature B lymphocytes. *J Biol Chem* 279: 20643–20654, 2004.
23. **Nam JH, Lee HS, Nguyen YH, Kang TM, Lee SW, Kim SJ, Kim HY, Earm YE, Kim SJ.** Mechanosensitive activation of K^+ channel via phospholipase C-induced depletion of PIP_2 in B lymphocytes. *J Physiol* 582: 977–990, 2007.
24. **Panyi G.** Biophysical and pharmacological aspects of K^+ channels in T lymphocytes. *Eur Biophys J* 34: 515–529, 2005.
25. **Panyi G, Vamosi G, Bodnar A, Gaspar R, Damjanovich S.** Looking through ion channels: recharged concepts in T-cell signaling. *Trends Immunol* 25: 565–569, 2004.
26. **Pottosin II, Bonales-Alatorre E, Valencia-Cruz G, Mendoza-Magaòa M, Dobrovinskaya OR.** TRESK-like potassium channels in leukemic T cells. *Pflügers Arch* 456: 1037–1048, 2008.
27. **Suh BC, Hille B.** PIP_2 is a necessary cofactor for ion channel function: how and why? *Annu Rev Biophys* 37: 175–195, 2008.
28. **Wulff H, Knaus HG, Pennington M, Chandy KG.** K^+ channel expression during B cell differentiation: implications for immunomodulation and autoimmunity. *J Immunol* 173: 776–786, 2004.
29. **Yun J, Kim S, Bang H.** TASK-1 channel promotes hydrogen peroxide induced apoptosis. *Korean J Physiol Pharmacol* 9: 63–68, 2005.
30. **Zheng H, Nam JH, Nguen YH, Kang TM, Kim TJ, Earm YE, Kim SJ.** Arachidonic acid-induced activation of large-conductance potassium channels and membrane hyperpolarization in mouse B cells. *Pflügers Arch* 456: 867–881, 2008.